A plane-wave pseudopotential study on III–V zinc-blende and wurtzite semiconductors under pressure

A plane-wave pseudopotential study on III–V zinc-blende and wurtzite semiconductors under pressure

S Q Wang and H Q Ye

Shenyang National Laboratory for Materials Science, Institute of Metal Research, Chinese Academy of Sciences, 72 Wenhua Road, Shenyang 110016, People's Republic of China

E-mail: sqwang@imr.ac.cn

Abstract
The results of a plane-wave pseudopotential study on the mechanical and electronic properties of twelve III–V zinc-blende (ZB) and wurtzite (WZ) semiconductors under pressure are presented. The lattice parameters, bulk moduli B_0, energy band types, band-gaps E_g^Γ at the Γ point, and pressure dependences of E_g^Γ are investigated in detail. Our results show that the E_g^Γ–P relations can be classified into two distinct types for these ZB and WZ phases. A transformation from one type of E_g^Γ–P relation to the other type is found to occur in some WZ phases. Linear relationships between the bulk moduli and the inverse of unit-cell volumes at $P = 0$ are also found for the ZB and WZ phases.

1. Introduction

Zinc-blende (ZB) and wurtzite (WZ) are the common structures of most group IV and III–V and many group II–VI semiconductors. The particular 'omni-triangulated' nature of the atomic structure gives these crystals unique mechanical and electronic properties. The pressure dependence of the photoluminescence of semiconductors is very useful in understanding the electronic energy band structure and structural properties. The effect of pressure on the electronic properties of III–V compounds can be investigated experimentally in many ways [1–5]. On the other hand, both theoretical and technical developments in density-functional-theory (DFT) and pseudopotential calculations in recent decades have provided researchers with powerful methods for predicting electronic and energetic properties as revealed by novel experimental techniques. Meanwhile, the technical development of epitaxial growth at the end of the last century has provided the possibility for researchers to fabricate synthetic materials with expected compositions and structures. The situation has stimulated extensive computational studies on high-pressure behaviour of various semiconductors [6–10].

In this work, we have performed a thorough DFT investigation of the nitrides, arsenides, phosphides, and antimonides of aluminium, gallium, and indium in both the ZB and WZ polytypes. The lattice parameters, bulk moduli, energy band structures, and their behaviours under pressure are calculated and analysed in detail.

2. The details of the DFT calculation

A plane-wave pseudopotential (PW-PP) scheme for solving the DFT equations in the local density approximation (LDA) is used in the present study. To achieve a highly efficient calculation without losing accuracy, Hartwigsen–Goedecker–Hutter (HGH) relativistic separable dual-space Gaussian pseudopotentials [11] within the LDA are employed in the calculation. The HGH pseudopotential is easy to use, as it is given in analytical form with only a few necessary parameters. The accuracy of the present implementation is verified by comparing with the relevant theoretical self-consistent linear muffin-tin orbital band structure calculations and LDA norm-conserving non-local pseudopotential calculations. The PW-PP calculations are realized using the ABINIT computer code[1].

The algorithms for volume optimization and full optimization of the cell geometry are used to obtain the optimal lattice constants of the ZB and WZ polytypes. These parameters are later compared with the lattice data from a Murnaghan fit of the equation of state (EOS), and the whole calculation repeated using the latter if necessary. Then, 41 sets of self-consistent DFT calculations are carried out with a well-distributed scaling of the cell dimensions from 0.98 to 1.02 in steps of 0.001, to generate the DFT ground state with its associated energy and density for each phase. At the end of the self-consistent calculation, a non-self-consistent calculation is performed to generate eigenenergies at 40 and 88 k-points respectively for the ZB and WZ phases for energy band structure analysis.

3. Lattice parameters and bulk moduli of III–V ZB and WZ phases

The theoretical lattice constants and bulk moduli in this section are obtained through fitting the 41 sets of DFT data for the potential curve with the Murnaghan EOS [12]:

$$E(V) - E(V_0) = \frac{B_0 V}{B_0'} \left[\frac{(V_0/V)^{B_0'}}{B_0' - 1} + 1 \right] - \frac{B_0 V_0}{B_0' - 1} \tag{1}$$

where $E(V)$ is the DFT ground-state energy with the cell volume V, V_0 is the unit-cell volume at zero pressure, B denotes the bulk modulus, and $B_0' = \partial B/\partial P$ at $P = 0$.

It had been verified that the Murnaghan EOS can both reproduce P–V data and yield correct values of the pressure bulk modulus for compressions up to about 10% (i.e. $V/V_0 > 0.9$) [13]. Hence, our results are reliable, since they involve using the Murnaghan EOS to calculate geometrical and mechanical parameters for the only $\pm 2\%$ volume variation in the present study.

3.1. Zinc-blende phases

Arsenides, phosphides, and antimonides of Al, Ga, and In generally take the ZB configuration at ambient conditions. Meta-stable ZB phases of GaN, AlN, and InN are also frequently observed, experimentally. The lattice parameters, bulk moduli, and band information for these phases from our PW-PP calculation are presented in table 1, where the first columns for a_0, B_0

Table 1. The lattice constants a_0, bulk moduli B_0, and band information for the twelve group III–V ZB phases. E_g^Γ is the band-gap at the Γ point. The band type is indicated by D and I, for direct and indirect energy band-gap, in the band information column, respectively.

	a_0 (nm)			B_0 (Mbar)					Band information	
	Present work	Other calculations	Experiment	Present work	Other calculations	Experiment	B_0'	E_g^Γ (eV)	Band type	
AlAs	0.5614	0.566 [15]	0.566 [20]	0.747		0.82 [20]	4.182	2.048	I	
AlN	0.4323	0.432 [16]	0.437 [21]	2.032	2.03 [16]		4.028	4.503	I	
AlP	0.5417	0.546 35 [17]	0.5467 [20]	0.886		0.86 [20]	4.037	3.261	I	
AlSb	0.6090	0.613 55 [15]	0.6136 [20]	0.561		0.58 [20]	4.362	1.670	I	
GaAs	0.5530	0.550 8 [18]	0.5649 [20]	0.757	0.771 [18]	0.77 [20]	4.487	1.008	D	
GaN	0.4335	0.444 6 [19]	0.450 [22]	2.070	2.01 [16]		4.136	3.211	D	
GaP	0.5322	0.535 8 [18]	0.5451 [23]	0.921	0.9783 [18]	0.88 [23]	4.339	2.438	I	
GaSb	0.5981	0.593 9 [18]	0.6081 [20]	0.567	0.7994 [18]	0.56 [20]	4.662	0.547	D	
InAs	0.5921	0.590 2 [18]	0.6054 [20]	0.617	0.6190 [18]	0.58 [20]	4.545	0.192	D	
InN	0.4801	0.492 [16]	0.498 [24]	1.476	1.39 [16]		4.060	0.753	D	
InP	0.5729	0.570 2 [18]	0.5867 [20]	0.736	0.7614 [18]	0.72 [20]	4.479	1.232	D	
InSb	0.6346	0.634 1 [18]	0.6472 [20]	0.476	0.4774 [18]	0.46 [20]	4.688	0.213	D	

and the column for B_0' give the data obtained from the Murnaghan fitting of the potential curve from the present PW-PP calculations. The next two columns for a_0, B_0 list the previously published theoretical and experimental data for comparison. The energy band-gap E_g^Γ at the Γ point is calculated from the fitted E_g^Γ–P quadratic equation at $P = 0$ (see section 5). The band type is determined by judging whether E_g^Γ is the minimum band-gap or not. Table 1 shows that $B_0' \sim 4$ for all twelve phases, which is consistent with previous results of EOS studies [14].

It can be seen from table 1 that the deviations between our PW-PP results and the experimental results are generally within 1% for a_0, and within 5% for B_0. All these errors are within the limitations of the PW-PP calculation. Our estimated band types are in accordance with the experiment results for all the known phases.

3.2. Wurtzite phases

GaN, AlN, and InN crystallize in the WZ structure at ambient conditions. WZ InP [25] and WZ GaP [26] are also often observed as meta-stable phases, experimentally. By choosing appropriate substrates under carefully controlled experimental conditions, it is feasible to use the molecular-beam epitaxy technique to grow films in both ZB and WZ polytypes for many compounds. A phase transition occurs from ZB to WZ at higher temperature for some ZB phases [27]. Like for ZB phases, our results for WZ phases are given in table 2. It is seen from tables 1 and 2 that the values of the bulk modulus for the two polytypes are quite close despite of the great differences in crystallographic structure. This result demonstrates that bulk modulus is a measure of bonding strength among local atoms, while there are the same local tetrahedrally bonded configurations in both ZB and WZ phases. The ZB polytypes of AlAs, AlN, and AlSb are all indirect band-gap semiconductors; however, they become direct band-gap semiconductors in the WZ form. This reflects the fact that the geometrical configuration plays an important role in the electronic properties of solids.

Table 2. Lattice constants, internal parameters u, bulk moduli B, and band information for the twelve group III–V WZ phases. E_g^Γ is the band-gap at the Γ point. The band type is indicated by D and I, for direct and indirect energy band-gap, in the band information column, respectively.

| | a_0 (nm) | | | u | c_0 (nm) | | | B_0 (Mbar) | | | | | Band information |
	Present work	Other calculations	Experiment	Present work	Present work	Other calculations	Experiment	Present work	Other calculations	Experiment	B_0'	E_g^Γ (eV)	Band type
AlAs	0.4001	0.3979 [28]		0.3791	0.6405	0.6497 [28]		0.7414			4.2080	1.5651	D
AlN	0.3077	0.3099 [28]	0.3112 [29]	0.3823	0.4923	0.4997 [28]	0.4982 [29]	2.0609	1.94 [43]	2.10 [37]	3.1401	4.6202	D
AlP	0.3837	0.3826 [28]		0.3760	0.6251	0.6286 [28]		0.8826			4.0448	2.2610	I
AlSb	0.4312			0.3751	0.7038			0.5555			4.3543	0.9524	D
GaAs	0.3912	0.3912 [28]		0.3747	0.6407	0.6441 [28]		0.7473			4.5048	0.7781	D
GaN	0.3066	0.3095 [28]	0.3189 [29]	0.3765	0.5005	0.5000 [28]	0.5185 [29]	2.0759	1.95 [43]	2.10 [37]	4.1965	3.3550	D
GaP	0.3763	0.3759 [28]		0.3744	0.6170	0.6174 [28]		0.9123			4.3437	1.4389	I
GaSb	0.4234			0.3749	0.6923			0.5580			4.6695	0.1673	D
InAs	0.4192			0.3755	0.6844			0.6098			4.5726	0.2051	D
InN	0.3406	0.3536 [28]	0.3548 [29]	0.3790	0.5499	0.5709 [28]	0.5760 [29]	1.4845		1.40 [37]	4.2538	0.9043	D
InP	0.4054			0.3750	0.6625			0.7306			4.4913	1.2696	D
InSb	0.4494			0.3750	0.7337			0.4690			4.6785	0.2172	D
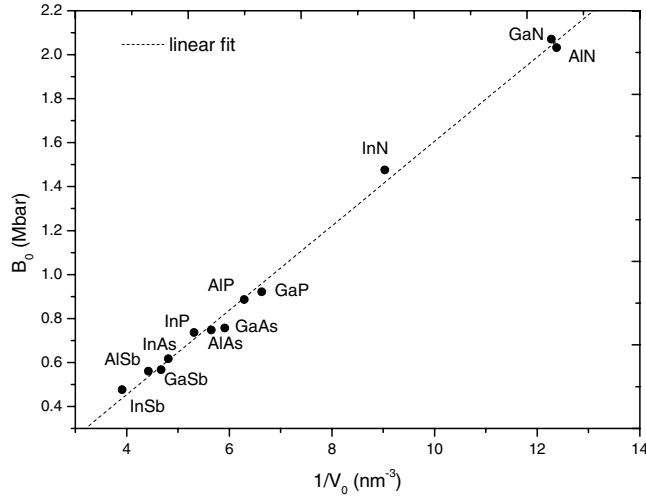
Figure 1. The B_0–$1/V_0$ relation for the twelve III–V ZB phases, showing a linear relationship between the two variables. The result of the linear fit is shown by the dashed line.

4. Relations between bulk modulus and cell dimension

The bulk modulus is a property of a material which defines its resistance to volume change when compressed. Both experimental and theoretical results suggest that the bulk modulus is a critical single-material property for indicating hardness, especially for cubic crystals. Bulk modulus is also an important parameter for the EOS of solids. By definition, the bulk modulus of solid material is given by

$$B_0 = -V \left(\frac{\partial P}{\partial V} \right)_T = -V \left(\frac{\partial^2 E}{\partial V^2} \right)_T \tag{2}$$

where B_0 is the bulk modulus at $P = 0$. The above equation hints at a close dependence of B_0 on V. In the following, we explore the relations between B_0 and the unit-cell volume V_0 for group III–V ZB and WZ phases on the basis of our theoretical PW-PP data.

The curves for B_0 as a function of the inverse of the cell volume V_0 are plotted in figures 1 and 2 for ZB and WZ phases, respectively, where V_0 is calculated as $V_0 = a_0^3$ for ZB phase and as $V_0 = \frac{\sqrt{3}}{2} a_0^2 c_0$ for WZ phase. It is immediately seen that there is a perfect linear relationship between B_0 and the inverse of V_0 for both polytypes. The following B_0–V_0 equation for the twelve ZB phases is obtained by a linear fitting of our theoretical data:

$$B_0 = -0.314\,63 + \frac{0.192\,05}{V_0}. \tag{3}$$

Similarly, the linear fit B_0–V_0 equation for the twelve WZ phases is given as

$$B_0 = -0.331\,38 + \frac{0.097\,35}{V_0}. \tag{4}$$

The coefficient of the $1/V_0$ term for the ZB phase in equation (3) is about double the coefficient for the corresponding WZ phase. Recalling that there are twice as many atoms in a unit cell of the ZB phase as in a unit cell of the WZ phase and that the unit-cell volume of the ZB phase is about double that of the WZ phase, one finally gets close values of the bulk moduli for the two polytypes.
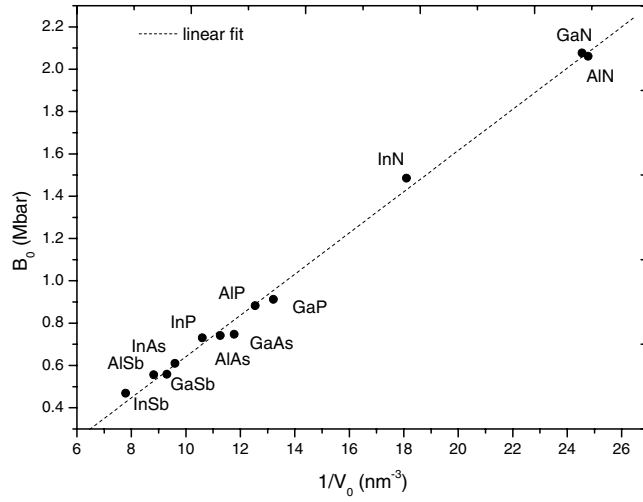
Figure 2. The B_0–$1/V_0$ relation for the twelve III–V WZ phases, showing a linear relationship between the two variables. The result of the linear fit is shown by the dashed line.

5. The pressure dependence of E_g^Γ

Photoluminescence spectra of semiconductors are sensitive to hydrostatic pressure. Theoretical investigation of the pressure dependence of the energy band structure provides a way to understand the chemical trends and dielectric behaviours of the compound. The results can be conveniently subjected to direct experimental verification. From the Murnaghan EOS, hydrostatic pressure is related to volume variation by

$$P = \frac{B_0}{B_0'}\left[\left(\frac{V_0}{V}\right)^{B_0'} - 1\right]. \tag{5}$$

The pressure dependence of E_g^Γ at the Γ point of the energy band for the ZB phase from the present energy band structure calculation is plotted in figure 3. Since the range of cell volume variation is $\pm 2.0\%$ for all phases in our energy band calculations, it is understood that hard material endures larger pressure before undergoing deformation and shows a longer line in the figure. One sees that all the E_g^Γ–P lines have the typical sublinear character. The slopes of all nitride E_g^Γ–P lines are smaller than for the other compounds. Antimonides are more sensitive to pressure (show much bigger slopes) due to their ultrasoftness. The situation is somewhat different for the E_g^Γ–P lines of the WZ phases, as shown in figure 4, where most of the line slopes are similar to those of the nitrides except for InAs, which is distinguished by a bigger slope. Furthermore, two-segment lines are found for InP, GaAs, and InSb. To explore the E_g^Γ–P relation quantitatively, the lines in figures 3 and 4 are analysed by means of linear fitting with the following equation:

$$E_g^\Gamma(P) = E_g^\Gamma(0) + kP \tag{6}$$

where $E_g^\Gamma(0)$ is the energy band-gap at the Γ point when $P = 0$ and is given in table 1 and 2 for the different phases. k is the pressure coefficient defined by $k = \mathrm{d}E_g^\Gamma/\mathrm{d}P$. The results of the linear fit are presented in table 3, where some other theoretical results and the data available from experiments are also listed. The WZ phases of GaAs, InP, and InSb are represented by two k-values, to correspond to the linear fit results for the first and the second parts of their E_g^Γ–P curves.
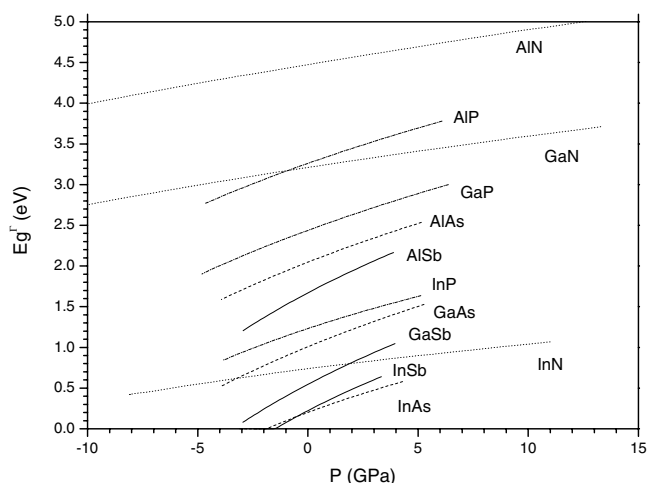
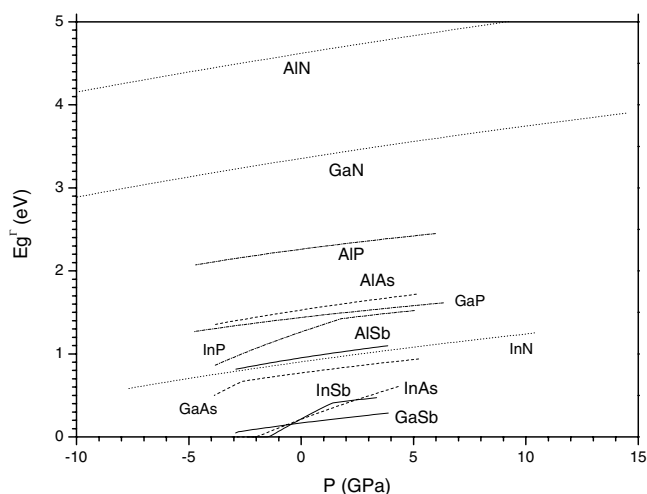**Figure 3.** The E_g^Γ–P curves of the twelve III–V ZB phases.

Figure 4. The E_g^Γ–P curves of the twelve III–V WZ phases. The E_g^Γ–P curves of AlN, GaN, and InN are similar to those in figure 3. Line bending can be seen for InSb, GaAs, and InP phases.

On comparing these pressure coefficients, one notices that astonishingly the pressure coefficients are nearly the same for nitrides in both ZB and WZ polytypes, while the coefficients for the rest of the ZB phases are about two to three times bigger than those for the corresponding WZ phases. The k-values of the first parts of the curves for WZ GaAs, InP, and InSb are close to the data for the ZB phases; the values for the second parts of the curves have the typical character of WZ phases. From these results it is concluded that the E_g^Γ–P relations of AlN, GaN, and InN always show the characters of the WZ phase no matter what the crystallographic structure is. The values of E_g^Γ for arsenides, phosphides, and antimonides in ZB phases are several times more sensitive to pressure than those for the corresponding WZ phases. Even in the WZ geometrical configuration, the E_g^Γ–P relations of GaAs, InP, and InSb undergo a transition from ZB-like character to WZ-like character at pressures of $P = -2.64$, 1.41, and 1.82 GPa, respectively. These strange behaviours of WZ GaAs, InP, and InSb are quite

Table 3. Pressure coefficients $k = \mathrm{d}E_g^\Gamma/\mathrm{d}P$ meV GPa^{-1} for the twelve III–V ZB and WZ semiconductors.

	Zinc-blende			Wurtzite		
	Present work	Other calculations	Experiment	Present work	Other calculations	Experiment
AlAs	104.5			40.6		
AlN	45.0	42.0 [8]		43.3	40.0 [8]	36.0 [33]
AlP	94.2			35.3		
AlSb	140.8			41.7		
GaAs	109.4	120.2 [39]	126.0 [36]	136.7, 34.3		
GaN	41.7	40.0 [8]		41.8	39.0 [8]	42.0 [31, 32], 41.4 ± 0.2 [40]
GaP	98.0	81.0 [35], 93.0 [30]	97.0 ± 0.8 [35]	31.1		
GaSb	140.3		145.0 [37]	34.1		
InAs	93.3	95.6 [6]	98.0 [3]	90.3		
InN	34.0	16.0 [8], 25.4 [6]		37.0	33.0 [8]	33.0 [34]
InP	88.4	78.1 [6]	85.0 [41], 92.5 [42]	99.4, 30.1		
InSb	132.7	136.7 [6]	128.0–155.0 [38]	144.7, 32.5		

interesting, and need further experimental verification. This unique pressure effect may have some application in microelectronics in the future.

6. Conclusions

We have presented theoretical results on lattice parameters, bulk moduli, and energy band structures of twelve III–V ZB and WZ phases. This work employed a first-principles PW-PP electronic structure calculation in the DFT LDA, using the HGH relativistic separable dual-space Gaussian pseudopotentials. We have correctly estimated the band type for all known phases by means of this realization. The calculated data for a_0, c_0, and B_0 have been compared with the available results, and an encouraging consistency found. We have explored the dependence of the bulk modulus on the cell dimension on the basis of our theoretical data. Linear relations between B_0 and the inverse of V_0 were found for both ZB and WZ phases. In studying the energy band properties under hydrostatic pressure, we found that the pressure coefficients $\mathrm{d}E_g^\Gamma/\mathrm{d}P$ can be divided into two categories: the ZB-like and WZ-like types. The usual pressure coefficient of the ZB phase is about two to three times that for the corresponding WZ phase. The nitrides of Al, Ga, and In have close pressure coefficients for both their ZB phases and their WZ phases and behave like WZ phases. Our theoretical results indicate a peculiar behaviour of the WZ phases of GaAs, InP, and InSb under pressure. Their E_g^Γ–P relations change from the ZB-like type to the WZ-like type at a certain hydrostatic pressure.

Acknowledgments

References

[1] Muller H, Trommer R, Cardona M and Vogl P 1980 *Phys. Rev.* B **21** 4879
[2] Menoni C, Hochheimer H and Spain I 1986 *Phys. Rev.* B **33** 5896

[3] Zallen R and Paul W 1967 *Phys. Rev.* **155** 703
[4] Pitt G 1973 *J. Phys. C: Solid State Phys.* **6** 1586
[5] Vohra Y, Weir S T and Ruoff A L 1985 *Phys. Rev.* B **31** 7344
[6] Van Camp P E, Van Doren V E and Devreese J T 1990 *Phys. Rev.* B **41** 1598
[7] Kim K, Lambrecht W R L and Segall B 1994 *Phys. Rev.* B **50** 1502
[8] Christensen N E and Gorczyca I 1994 *Phys. Rev.* B **50** 4397
[9] Kelsey A A and Ackland G J 2000 *J. Phys.: Condens. Matter* **12** 7161
[10] Tsai M H, Dow J D and Kasowski R V 1996 *J. Mater. Res.* **7** 2205
[11] Hartwigsen C, Goedecker S and Hutter J 1998 *Phys. Rev.* B **58** 3641
[12] Murnaghan F D 1944 *Proc. Natl Acad. Sci. USA* **30** 244
[13] Murnaghan F D 1937 *Am. J. Math.* **49** 235
[14] Jeanloz R 1988 *Phys. Rev.* B **38** 805
[15] Palmer D W 2000 webpage www.semiconductors.co.uk 11
[16] Kim K, Lambrecht W R L and Segall B 1996 *Phys. Rev.* B **53** 16 310
[17] Singh J 1993 *Physics of Semiconductors and their Heterostructures* (New York: McGraw-Hill)
[18] Kalvoda S, Paulus B and Fulde P 1997 *Phys. Rev.* B **55** 4027
[19] Logothetidis S, Petalas J, Cardona M and Moustakas T D 1994 *Phys. Rev.* B **50** 18 017
[20] Hellwege K H and Madelung O 1982 *Landolt–Börnstein New Series* Group III, vol 17a (Berlin: Springer)
[21] Edgar J H 1994 *Properties of Group III Nitrides (Electronic Materials Information Service (EMIS) Datareviews Series)* (London: Institution of Electrical Engineers)
[22] Lei T, Moustakas T D, Graham R J, He Y and Berkowitz S J 1992 *J. Appl. Phys.* **71** 4933
[23] Levinstein M, Rumyantsev S and Shur M 1999 *Handbook Series on Semiconductor Parameters* vols 1, 2 (London: World Scientific)
[24] Strite S, Ruan J, Smith D J, Sariel J, Manning N and Chen H 1992 *Bull. Am. Phys. Soc.* **37** 346
[25] Gaiduk P I, Komarov F F, Tishkov V S, Wesch W and Wendler E 2000 *Phys. Rev.* B **61** 15 785
[26] Narayanan V, Mahajan S, Sukidi N, Bachmann K J, Woods V and Dietz N 2000 *Phil. Mag.* A **80** 555
[27] Qadri S B, Skelton E F, Hsu D, Dinsmore A D, Yang J, Gray H F and Ratna B R 1999 *Phys. Rev.* B **60** 9191
[28] Yeh C Y, Lu Z W, Froyen S and Zunger A 1992 *Phys. Rev.* B **46** 10 086
[29] Strite S and Morkoc H 1992 *J. Vac. Sci. Technol.* B **10** 1237
[30] Blacha A, Presting H and Cardona M 1984 *Phys. Status Solidi* b **126** 500
[31] Morkoc H, Strite S, Gao G B, Lin M E, Sverdlov B and Burns M 1994 *J. Appl. Phys.* **76** 1363
[32] Akasaki I and Amano H 1994 *J. Electrochem. Soc.* **141** 2266
[33] Gorczyca I and Christensen N E 1993 *Physica* B **185** 410
[34] Perlin P, Iota V, Weinstein B A, Wisniewski P, Suski T, Eliseev P G and Osinski M 1997 *Appl. Phys. Lett.* **70** 2993
[35] Ves S, Strossner K, Kim C K and Cardona M 1985 *Solid State Commun.* **55** 327
[36] Welber B, Cardona M, Kim C K and Rodriguez S 1975 *Phys. Rev.* B **12** 5729
[37] Levinstein M, Rumyantsev S and Shur M 1996 *Handbook Series on Semiconductor Parameters* vol 1 (London: World Scientific)
[38] Booth I, Hawton M and Keller W 1982 *Phys. Rev.* B **25** 7713
[39] Christensen N E 1984 *Phys. Rev.* B **30** 5753
[40] Perlin P, Mattos L, Shapiro N A, Kruger J, Wong W S, Sands T, Cheung N W and Weber E R 1999 *J. Appl. Phys.* **85** 2385
[41] Tsay T, Mita S and Bendow B 1974 *Phys. Rev.* B **10** 1476
[42] Kobayashi T, Aoki K and Yamamoto K 1986 *Physica* B + C **139–140** 537
[43] Miwa K and Fukumoto A 1993 *Phys. Rev.* **48** 7897